

Queen Mary, University of London
School of Mathematical Sciences

MTH6138 : Third Year Project

Fractal Concepts and the Coastline

Mariam Yusuf Ahmed

170993146

Supervisor: Dr Wolfram Just

Abstract

Acknowledgements

I am grateful to my supervisor Dr Wolfram Just, who always eased my worries and motivated me throughout this thesis, especially considering the current climate.

Contents

1	Introduction	4
2	Dimension^[1]	5
2.1	Box-counting Dimension	5
2.1.1	Definitions	5
2.1.2	Mathematical concept of dimension	5
2.2	Middle third Cantor Set	5
2.2.1	Dimension of the Cantor Set	6
2.3	The Von Koch Curve	6
2.3.1	Dimension of the Koch Curve	8
2.4	The Sierpinski Triangle	8
2.4.1	Dimension of the Sierpinski Triangle	10
2.5	Limitations of dimension ^[4]	10
3	Self-Similarity	10
3.1	Definitions ^[3]	10
3.2	Self-similarity of the Cantor set	11
3.3	Self-similarity of the Sierpinski Triangle	11
3.4	Self-similarity of the Koch curve ^[3]	12
4	The Coastline^[7]	12
4.1	Background information	12
4.2	The Richardson Effect	12
4.3	Modelling the Coastline ^[6]	14
4.3.1	The Koch curve	14
4.3.2	Random walks and Brownian motion ^{[5][6]}	14
5	Iterated function systems	16
5.1	Background Information ^[2]	16
5.2	Definitions ^[2]	16
5.3	Iterated function system of the Koch Curve ^[8]	16
5.4	Iterated function system of the Koch Snowflake ^[9]	17
5.5	Iterated function system of the Sierpinski Triangle ^[11]	20
5.6	Iterated function system of the Sierpinski Carpet ^[10]	21
6	Conclusion	23
	Bibliography	24

1 Introduction

Geometry, tracing back to ancient Egypt, is a branch of mathematics concerned with shapes and sizes. However, it is often concentrated on smooth and regular objects such as circles, cubes and cones. Similarly, Calculus, which was developed in the 17th century by Newton and Leibniz, is used to analyse smooth objects. As a result, many natural phenomena were historically considered too irregular and complex to be described using traditional mathematical concepts. In the late 1960s Benoit Mandelbrot coined the term ‘fractals’ to describe a large class of irregular objects. He also went on to describe numerous fractal concepts in his book ‘The Fractal Geometry of Nature’ and he was often referred to as ‘the Father of Fractals’. In this thesis I will describe different terms such as ‘Dimension’ and ‘Self-similarity’ as well as highlighting relevant examples; the Koch curve, the Sierpinski triangle, and the middle third Cantor set.

Alongside the theoretical nature of fractal geometry, fractals also appear in the real world, often without us even noticing. Fractal networks can be found in the human body, within our respiratory system and blood vessels and they are prevalent in the atmosphere through the formation of clouds. There is also some research that suggests that the universe itself has some sort of hierarchical structure. In my thesis I will focus on the fractal geometry of the coastline. In particular, I will describe the research carried by Mandelbrot and scientist Lewis Fry Richardson who sought to find a method to measure the coastline. I will also introduce the concept of iterated function systems, which can be used to construct fractal structures.

2 Dimension_[1]

2.1 Box-counting Dimension

2.1.1 Definitions

Box-counting dimension: Let S be a bounded subset of \mathbb{R}^n , we set $N(S, \epsilon)$ to be the number of boxes of side length ϵ needed to cover S . The *box-counting dimension* (also known as the Minkowski-Bouligand dimension) of S is formally defined to be

$$\dim(S) = \lim_{\epsilon \rightarrow 0} \frac{\ln(N(S, \epsilon))}{\ln(1/\epsilon)}$$

This definition is valid only if the limit exists. In cases where the limit doesn't exist, we use a more technical definition known as the Hausdorff dimension, which always exists for a bounded set of \mathbb{R}^n .

2.1.2 Mathematical concept of dimension

When referring to dimension, we are often working on the Euclidean space which is 3-dimensional. Any value we obtain will therefore lie between 0 and 3, where a dimension of 0 represents a point, a dimension of 1 represents a line, a dimension of 2 represents a plane and if the dimension is 3, this represents a sphere.

Initially, it may seem difficult to assign a dimension to a set S , where $S \subset \mathbb{R}^n$. We therefore consider the case when S is a curve in \mathbb{R}^2 , and we assume that $S \subset I \times I$ (unit square). We then divide the unit square into n^2 little squares, with each side measuring at a length of $\epsilon = \frac{1}{n}$. We let $N_n = N_\epsilon$ be the number of squares of side length $\epsilon = \frac{1}{n}$ which intersect S . We then find that, for a smooth curve S , $N_n \sim n$ as $n \rightarrow \infty$.

Conversely, if S was a 2-dimensional shape such as a circle, then the number of little squares that it meets would be roughly $N_n \sim n^2$ as $n \rightarrow \infty$.

Essentially, for a fractal S , we say that S has a dimension d if the number of little squares that S meets is proportional to $N_n \sim n^d = \left(\frac{1}{\epsilon}\right)^d$ as $n \rightarrow \infty$.

2.2 Middle third Cantor Set

Take a unit length polygon and split it into three equal parts. We then remove the middle third, we are now left with two smaller polygons. In the box-counting dimension equation, ϵ represents the length of the intervals, and $N(S, \epsilon)$ represents the number of intervals.



Figure 1: Cantor Set

2.2.1 Dimension of the Cantor Set

For the first line shown in the Cantor set diagram, $\epsilon = 1$, for the second line $\epsilon = 1/3$, for the third line $\epsilon = 1/3^2$, and for the fourth line $\epsilon = 1/3^3$, and this continues with the value of ϵ getting smaller each time. After n iterations, $\epsilon = 1/3^n$.

We then substitute the ϵ values found above into $N(S, \epsilon)$. The number of intervals in the first line of the Cantor set is now $N(C, 1) = 1$, the second line is $N(C, 1/3) = 2$, the third line is $N(C, 1/3^2) = 2^2 = 4$ and the fourth line is $N(C, 1/3^3) = 2^3 = 8$. The number of values continues to increase, after n iterations $N(C, 1/3^n) = 2^n$. Hence,

$$Dim(C) = \lim_{n \rightarrow \infty} \frac{\ln(N(C, \frac{1}{3^n}))}{\ln(\frac{1}{3^n})} = \lim_{n \rightarrow \infty} \frac{\ln(2^n)}{\ln(3^n)} = \frac{\ln(2)}{\ln(3)} = \log_3 2 \simeq 0.6309$$

2.3 The Von Koch Curve

Consider a straight line that has been split into three equal parts, each with a length of a third.



Figure 2: Straight line with 3 equal parts

We then replace the middle third of the line by the other sides of an equilateral triangle with side length $1/3$. The length of the curve formed has increased and the curve is now as follows:



Figure 3: Straight line with the middle third removed



Figure 4: First Iteration of the Koch Curve

We then repeat the same steps, this results in the following iterations:

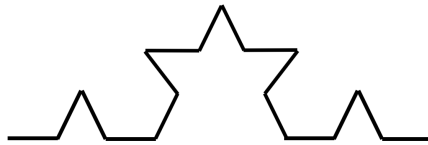


Figure 5: Second Iteration of the Koch Curve

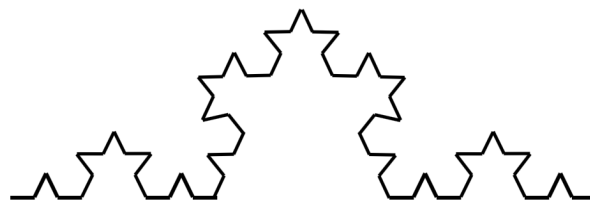


Figure 6: Third Iteration of the Koch Curve

After infinite iterations, the length of the Koch curve is infinite:

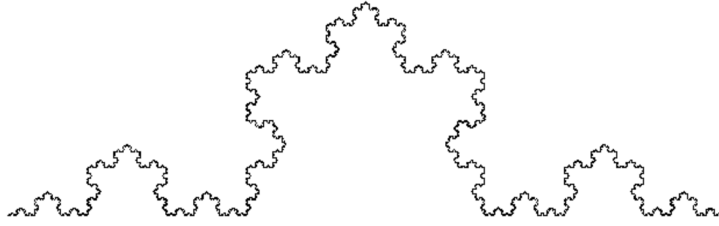


Figure 7: Koch Curve

2.3.1 Dimension of the Koch Curve

In the diagrams of the Koch curve shown above, the length increases at each iteration. In the original line split into 3, the length stands at 1. After the first iteration, there are 4 thirds and the length is $4/3$. After the second iteration the length is $(4/3)^2$. Continuing the trend, the length after n iterations is $(4/3)^n$. Thus, as the value of n increases, the length of the Von Koch curve tends to infinity.

To calculate the dimension of the Von Koch curve, we cover the curve with triangles of side length $1/3^n$. We first use 1 triangle of side length $1/3^0 = 1$, which gives $N(S, 1) = 1$. We next use 4 triangles of side length $1/3$ which gives $N(S, \frac{1}{3}) = 4$. In the next step we use 4^2 triangles of side length $1/3^2$, which gives $N(S, \frac{1}{3^2}) = 4^2$. Inductively, after n steps, we use 4^n triangles of side length $1/3^n$, to give $N(S, \frac{1}{3^n}) = 4^n$. Hence,

$$Dim(S) = \lim_{n \rightarrow \infty} \frac{\ln(N(S, \frac{1}{3^n}))}{\ln(1/\frac{1}{3^n})} = \lim_{n \rightarrow \infty} \frac{\ln(4^n)}{\ln(3^n)} = \frac{\ln(4)}{\ln(3)} = 2 \log_3 2 \simeq 1.2618$$

2.4 The Sierpinski Triangle

Consider an equilateral triangle, that has been divided into 4 smaller equilateral triangles. We remove the middle triangle, which creates a triangle hole and we are now left with 3 equilateral triangles. As we repeat the steps, the area of the triangle decreases and after infinite iterations, the area tends to zero.

The process is illustrated below:

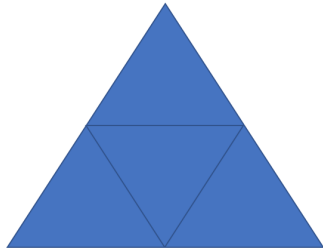


Figure 8: Equilateral triangle divided into 4 parts

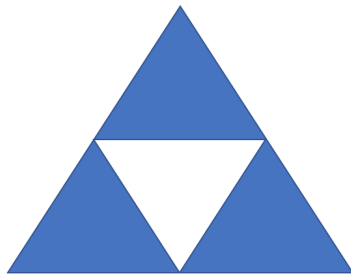


Figure 9: First iteration of the Sierpinski Triangle

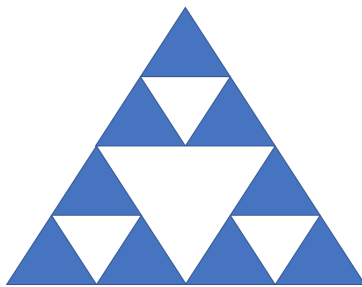


Figure 10: Second iteration of the Sierpinski Triangle

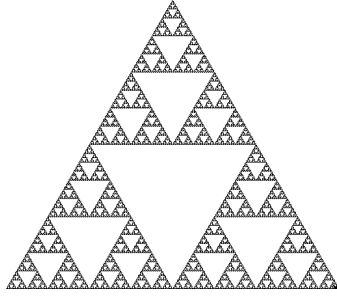


Figure 11: The Sierpinski Triangle

2.4.1 Dimension of the Sierpinski Triangle

To calculate the dimension of the Sierpinski triangle, we use 3 squares with $\epsilon = 1/2$. In Figure 8, $\epsilon = 1$ and since there's only one square, $N(S, 1) = 1$. After the first iteration of the Sierpinski triangle, $N(S, \frac{1}{2}) = 3$, and after the second iteration, $N(S, \frac{1}{4}) = 3^2$. Inductively, $N(S, \frac{1}{2^n}) = 3^n$. Hence,

$$Dim(S) = \lim_{n \rightarrow \infty} \frac{\ln(N(S, \frac{1}{2^n}))}{\ln(1/\frac{1}{2^n})} = \lim_{n \rightarrow \infty} \frac{\ln(3^n)}{\ln(2^n)} = \frac{\ln(3)}{\ln(2)} = \log_2 3 \simeq 1.58496$$

2.5 Limitations of dimension^[4]

Although the dimension of fractals provide information about how they appear under magnification, dimension provides limited information about objects that come in different shapes or forms. In fact, some fractals may have the same dimension, but a completely different structure. For instance, a fractal with a dimension of 1.26 could represent a variety of different objects. It may be the dimension of a continuous object like the Von Koch curve, or be disconnected with many intervals, similar to the Cantor set. Topology can be used to further explain this concept. Another limitation of dimension is that it doesn't tell us much about the 'texture' of fractals. Lacunarity and porosity are ideas that can be instead used to describe texture.

3 Self-Similarity

3.1 Definitions^[3]

Similar: Two figures on a plane are *similar* if they have the same shape but not necessarily the same size. One figure may be obtained from the other by scaling, re-positioning, rotating or by flipping it over.

Self-Similar: A *self-similar* set is one that is made up of several smaller similar copies of itself.

3.2 Self-similarity of the Cantor set

If we take the second line of the Cantor set diagram shown in figure 1, we can see that it consists of two parts. The left hand side is from 0 to $1/3$ and the right hand side is from $2/3$ to 1. If we consider the left hand side and scale it by multiplying it by a factor of 3, we are now left with a line from 0 to 1. Hence, the function $f_1(x) = 3(x)$ directly transforms the line into the full Cantor set $[0,1]$.

Similarly, if we now take the right hand side $[\frac{2}{3}, 1]$ and scale it by applying the function $f_2(x) = 3(x - \frac{2}{3})$, the $2/3$ becomes 0 and the 1 value remains the same. Thus, $[\frac{2}{3}, 1]$ is now mapped to $[0,1]$, the full Cantor set.

Therefore, the two functions described above, $f_1(x) = 3(x)$ and $f_2(x) = 3(x - \frac{2}{3})$, both characterise self-similarity by definition; each iteration of the Cantor set is made up of smaller similar copies of the full Cantor set. After infinite iterations, a set containing infinitely many disjointed points (polygons) will form. This is known as Cantor Dust.

3.3 Self-similarity of the Sierpinski Triangle

If we take Figure 11 which illustrates the final Sierpinski triangle, we can demonstrate self-similarity. The Sierpinski triangle is made up of 3 smaller triangles. If we take the triangle on the bottom left, we can map it to the full Sierpinski triangle by the function $f_1(x, y) = (2x, 2y)$, where x represents the base of the triangle and y represents the vertical height.

In a like manner, if we take the the bottom right triangle and apply the same function $f_1(x, y) = (2x, 2y)$, we will again obtain the Sierpinski triangle. However, we also need to translate the triangle to the left. Hence, we use the function $f_2(x, y) = (2(x - \frac{1}{2}), 2y)$.

Finally, for the top triangle, we need to scale the triangle in the same way and also translate it by shifting it down and to the left. We therefore use the function $f_3(x, y) = (2(x - \frac{1}{4}), 2(y - \frac{\sqrt{3}}{4}))$. Hence in this case, self-similarity is expressed by the three functions $f_1(x, y), f_2(x, y), f_3(x, y)$.

3.4 Self-similarity of the Koch curve^[3]

The Koch curve is self-similar since it comprises 4 scale $1/3$ copies of itself. This can be represented in a diagram with a template consisting of a large rectangle and 4 smaller rectangles, each a $1/3$ scale copy of the large one. The said template is shown below.

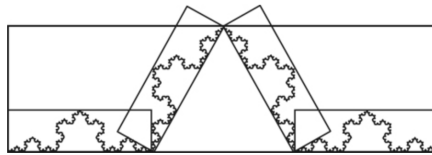


Figure 12: The von Koch curve together with its defining template^[3]

4 The Coastline^[7]

4.1 Background information

Typically, length is measured by the distance between the beginning and end of a straight line. In terms of a coastline, measuring the length is much harder due to its irregular and winding nature. The length would therefore be considerably longer than the distance between the start and end points of said coastline. All measurement methods used to evaluate the length suggest that the typical coastline's length is so ill determined that it is considered infinite. Fractal concepts of dimension, measure and curve are therefore introduced.

In 'The Fractal Geometry of Nature', Benoit Mandelbrot describes different methods of measurement that have been used in attempt to measure the length of the coastline. The first method, described as method A, consisted of setting dividers to a prescribed opening ϵ and walking the dividers along the coastline. The number of steps multiplied by ϵ provides a length $L(\epsilon)$ which was expected to settle at a value defined as the 'true length'. However, due to the irregularity of the coastline, the observed $L(\epsilon)$ increased without limit. The same conclusion is evident for the other methods highlighted; the estimated length tends to increase without limit.

4.2 The Richardson Effect

Mandelbrot also describes how $L(\epsilon)$ obtained in method A, has been studied in Richardson 1961. Richardson was a scientist who was responsible for

ideas regarding the nature of turbulence as well as other difficult problems, including the nature of armed conflict between states. Richardson performed experimental measurements of length on various curves using equal sided polygons of increasingly short side ϵ . As expected, the increasingly precise measurements made on a circle stabilised rapidly near a well-determined value.

Richardson studied coastal length in many different countries. Using the definition of $L(\epsilon)$ and the idea that $L = \lim_{\epsilon \rightarrow \infty} L(\epsilon)$, Richardson discovered that for each length, the number of sections at scale ϵ satisfied the empirical law $N(\epsilon) = K\epsilon^{-D}$, where K and D are constants specific to the different countries.

Mandelbrot further describes how Richardson found that in the case of coastlines, the approximate lengths do not stabilise. As the yardstick length ϵ approaches zero, the lengths, on a logarithmic plot, fall on a straight line of a negative slope. This is known as the Richardson Effect and is illustrated in the figure below:

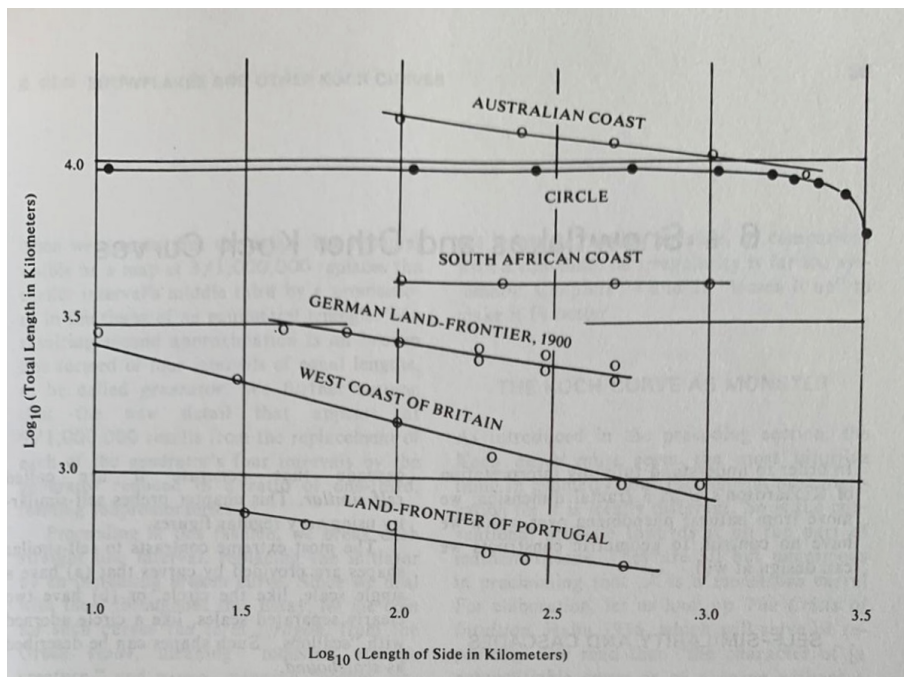


Figure 13: Richardson’s empirical data on the rate of increase of coastlines lengths^[7]

Richardson measured coastlines on maps by using different step lengths, in order to get an estimate of the total length. As shown in figure 13, the

slopes for the different lengths vary. We can see that for a circle, the slope is flat with a gradient of 0 when the side length is less than 2.75km. Similarly, the slope for the South African coast is also close to 0, which suggests that it has a ‘smooth’ nature. On the other hand, the west coast of Britain has a rather steep slope, with a gradient of about 0.25, which indicates that it appears to be more ‘rough’. These findings demonstrate the ‘fractality’ of the coastline. Mandelbrot’s analysis of Richardson’s data led to the idea that the coastline is statistically self-similar.

Richardson’s empirical data led him to conclude that in order to measure the coastline length, $N_E \simeq \lambda E^{1-D}$ elements are required, where λ represents a constant. If we take the logarithm of each side of the equation, we get:

$$\log N_E \simeq \log \lambda E^{1-D} \simeq \log \lambda + \log E^{1-D} \simeq (1 - D) \log E + \log \lambda$$

This equation could be used to plot a log-log graph, where the value for λ is specific to each coastline. Then, by finding an approximate value for the length of connected physical curves, we would be able to estimate the dimension of a coastline. For example, a careful analysis of the coastline of Britain found that its fractal dimension is 1.25.

4.3 Modelling the Coastline_[6]

4.3.1 The Koch curve

The self-similarity of the Koch curve has enabled it to serve as a good mathematical model of the coastline. However in some aspects, it fails to accurately represent coastlines. The sequence of scales in the Koch curve are in powers of $\frac{1}{3}$, therefore examining the curve at different intervals e.g. $\frac{1}{4}$, would no longer show self-similarity. Also, despite the irregularity of the Koch curve, its structure is ordered, unlike the coastline. These limitations can be diminished by randomising the fractals.

4.3.2 Random walks and Brownian motion_{[5][6]}

A ‘random walk’ is a concept that leads to fractal graphs and objects. A walker sets off from an origin point at a time 0, and takes a step of 1 unit each second, either forwards or backwards. The chosen direction is picked at random with a 50/50 chance of the walker going in either direction. Since the walker’s movements are random, they generally do not make much progress in each direction and it will take quite some time for the walker to have travelled far from the origin. Therefore, the graph of a random walk is very irregular, as illustrated below:

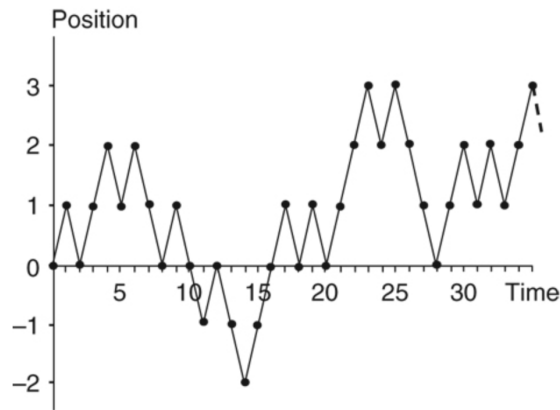


Figure 14: The progress of a typical random walk^[5]

If the walker was to take shorter, but more frequent steps, the graph would appear to have a similar overall structure, but it would be more irregular when viewed at a smaller scale. The graph of the random walk now takes on a fractal form called the ‘Brownian process’. Taking very short steps very quickly, gives *spatial* Brownian motion.

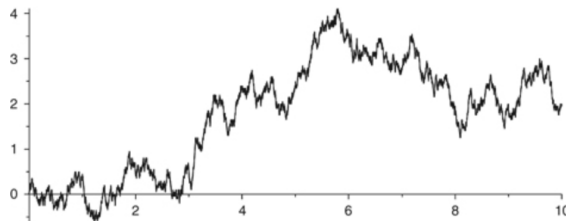


Figure 15: The Brownian process^[5]

Brownian motion in a plane can be generated by a random walk through a square lattice, where at each time interval there is an equal chance of movement in any direction. The path created through Brownian motion is said to have a dimension of 2. This suggests that the path will be very irregular with many self-intersections, unlike the coastline which tends to have no self-intersections.

Mandelbrot therefore rediscovered *fractional* Brownian motion while searching for an improved self-similar model of the coastline. The movement of a particle under fractional Brownian motion generally tends to persist in a motion which results in fewer self-intersections and generates fractal curves of

greater regularity, similar to coastlines. Mandelbrot named the tendency of particles to persist over time, the ‘Joseph Effect’.

5 Iterated function systems

5.1 Background Information_[2]

The self-similarity of fractals can be used to define them using iterated function systems. These systems can often lead to a simple way of finding the dimension of a fractal.

First we let D be a closed subset of \mathbb{R}^n . A mapping $S : D \rightarrow D$ is defined as a contraction on D if there exists a number k with $0 < k < 1$ such that $|S(x) - S(y)| \leq k|x - y|$ for all $x, y \in D$. By this definition, any contraction is continuous. If $|S(x) - S(y)| = k|x - y|$, then S is a transformation that maps sets into similar sets. Hence, S is contracting similarity.

5.2 Definitions_[2]

Iterated Function System: A finite set of contractions $\{S_1, S_2, \dots, S_n\}$ where $n \geq 2$ is called an *iterated function system*.

Attractor: A non-empty subset F of D is known as an *attractor (or invariant set)* of the iterated function system if

$$F = \bigcup_{i=1}^n S_i(F)$$

provided that it consists of its images under the S_i .

5.3 Iterated function system of the Koch Curve_[8]

If we take the first iteration of the Koch curve, we can see that the curve comprises of four copies of the unit horizontal line, with each segment scaled by $\frac{1}{3}$. The two middle segments are also each rotated by 60° , with the left side being rotated anti-clockwise and the right side rotated clockwise. This is illustrated in the diagram below:

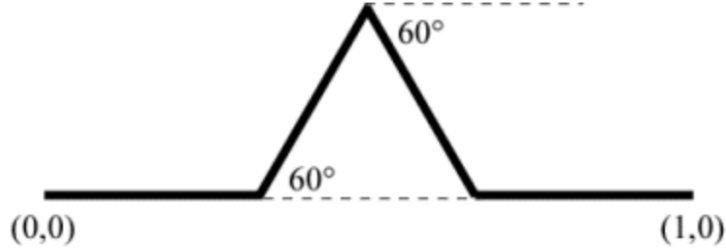


Figure 16: Koch Curve_[8]

Alongside the translations to the four segments of the Koch curve, this yields the following iterated function system:

$$f_1(x) = \begin{bmatrix} \frac{1}{3} & 0 \\ 0 & \frac{1}{3} \end{bmatrix} x \quad \text{scaled by } \frac{1}{3}$$

$$f_2(x) = \begin{bmatrix} \frac{1}{6} & -\frac{\sqrt{3}}{6} \\ \frac{\sqrt{3}}{6} & \frac{1}{6} \end{bmatrix} x + \begin{bmatrix} \frac{1}{3} \\ 0 \end{bmatrix} \quad \text{scaled by } \frac{1}{3} \text{ and rotated by } 60^\circ$$

$$f_3(x) = \begin{bmatrix} \frac{1}{6} & \frac{\sqrt{3}}{6} \\ -\frac{\sqrt{3}}{6} & \frac{1}{6} \end{bmatrix} x + \begin{bmatrix} \frac{1}{3} \\ \frac{\sqrt{3}}{6} \end{bmatrix} \quad \text{scaled by } \frac{1}{3} \text{ and rotated by } -60^\circ$$

$$f_4(x) = \begin{bmatrix} \frac{1}{3} & 0 \\ 0 & \frac{1}{3} \end{bmatrix} x + \begin{bmatrix} \frac{2}{3} \\ 0 \end{bmatrix} \quad \text{scaled by } \frac{1}{3}$$

The Koch curve is the fixed attractor of this iterated function system.

5.4 Iterated function system of the Koch Snowflake_[9]

For the Koch snowflake, we start with an equilateral triangle $T=K(0)$. We then scale T by a factor of $\frac{1}{3}$ and position 3 copies of the triangles across the sides of the triangle to form $K(1)$. For the second iteration, we scale T by $(\frac{1}{3})^2 = \frac{1}{9}$ and position 12 copies of the triangle along $K(1)$ to produce $K(2)$. Next, we scale T by $(\frac{1}{3})^3 = \frac{1}{27}$ and position 48 copies of T along $K(2)$ to

generate the image of $K(3)$. After infinite iterations, the Koch snowflake is formed, this process is illustrated below:

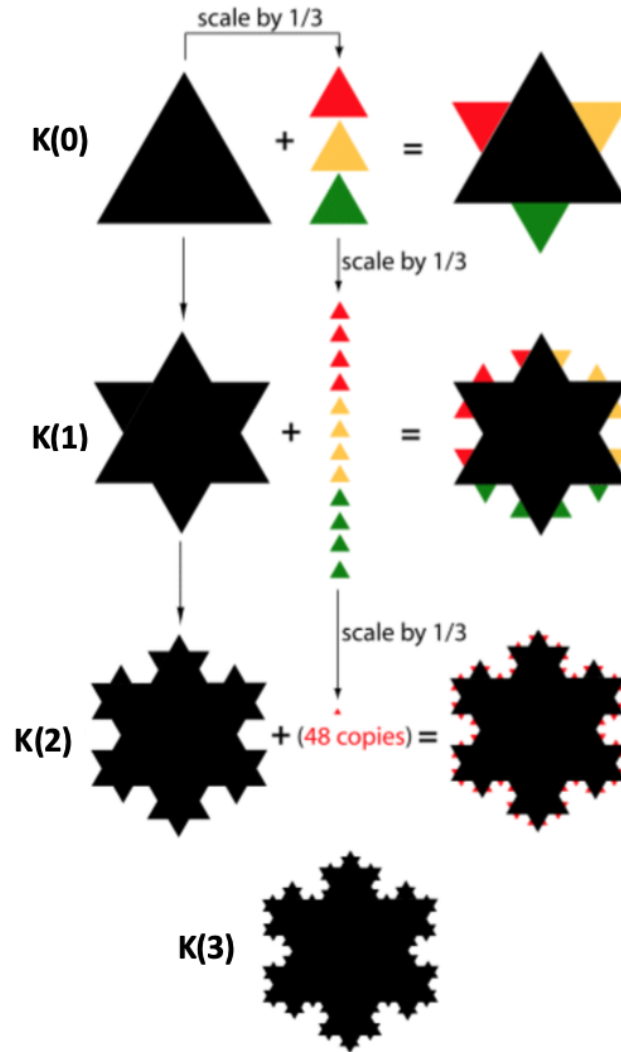


Figure 17: Koch Snowflake^[9]

An example of an iterated function system for the snowflake is shown below, it is based on the scaling of hexagons.

$$f_1(x) = \begin{bmatrix} \frac{1}{2} & -\frac{\sqrt{3}}{6} \\ \frac{\sqrt{3}}{6} & \frac{1}{2} \end{bmatrix} x \quad \text{scaled by } \frac{1}{3} \text{ and rotated by } 30^\circ$$

$$f_2(x) = \begin{bmatrix} \frac{1}{3} & 0 \\ 0 & \frac{1}{3} \end{bmatrix} x + \begin{bmatrix} \frac{1}{\sqrt{3}} \\ \frac{1}{3} \end{bmatrix} \quad \text{scaled by } \frac{1}{3}$$

$$f_3(x) = \begin{bmatrix} \frac{1}{3} & 0 \\ 0 & \frac{1}{3} \end{bmatrix} x + \begin{bmatrix} 0 \\ \frac{2}{3} \end{bmatrix} \quad \text{scaled by } \frac{1}{3}$$

$$f_4(x) = \begin{bmatrix} \frac{1}{3} & 0 \\ 0 & \frac{1}{3} \end{bmatrix} x + \begin{bmatrix} \frac{-1}{\sqrt{3}} \\ \frac{1}{3} \end{bmatrix} \quad \text{scaled by } \frac{1}{3}$$

$$f_5(x) = \begin{bmatrix} \frac{1}{3} & 0 \\ 0 & \frac{1}{3} \end{bmatrix} x + \begin{bmatrix} \frac{-1}{\sqrt{3}} \\ \frac{-1}{3} \end{bmatrix} \quad \text{scaled by } \frac{1}{3}$$

$$f_6(x) = \begin{bmatrix} \frac{1}{3} & 0 \\ 0 & \frac{1}{3} \end{bmatrix} x + \begin{bmatrix} 0 \\ \frac{-2}{3} \end{bmatrix} \quad \text{scaled by } \frac{1}{3}$$

$$f_7(x) = \begin{bmatrix} \frac{1}{3} & 0 \\ 0 & \frac{1}{3} \end{bmatrix} x + \begin{bmatrix} \frac{1}{\sqrt{3}} \\ \frac{-1}{3} \end{bmatrix} \quad \text{scaled by } \frac{1}{3}$$

The iterated function system described, produces an attractor that consists of a copy of the Koch snowflake scaled by $\frac{1}{\sqrt{3}}$ and 6 smaller copies scaled by $\frac{1}{3}$. This is illustrated below:

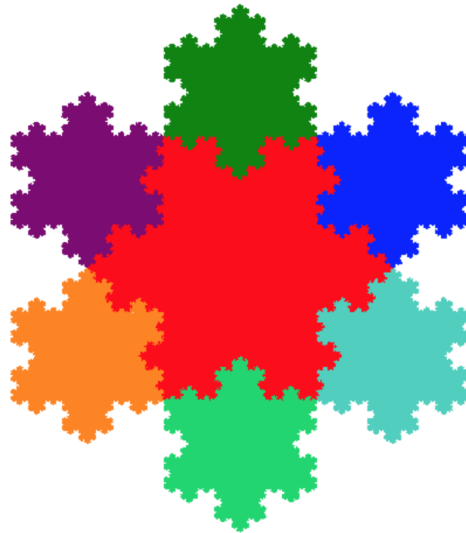


Figure 18: Koch Snowflake Attractor^[9]

5.5 Iterated function system of the Sierpinski Triangle_[11]

As previously mentioned, for the Sierpinski triangle we divide an equilateral triangle into four smaller equilateral triangles. The midpoint of each side of the original triangle is used as the new vertices. After removing the middle triangle, we repeat this step with the remaining three triangles. As we continue repeating the steps we obtain a decreasing sequence of sets. If we label our equilateral triangle $S(0)$, and the first, second and third iterations, $S(1)$, $S(2)$ and $S(3)$ respectively, we have: $S(0) \supset S(1) \supset S(2) \supset S(3) \supset \dots$

The first iteration $S(1)$ can also be obtained by scaling three copies of $S(0)$ by $\frac{1}{2}$ and translating the three triangles into an arrangement that is the same shape as $S(0)$. The vertices of the triangle are as follows:

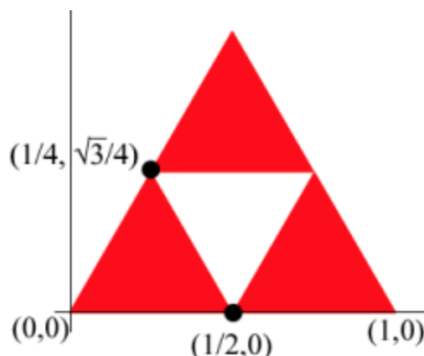


Figure 19: Vertices of the 1st iteration of the Sierpinski Triangle_[11]

This yields the following iterated function system:

$$f_1(x) = \begin{bmatrix} \frac{1}{2} & 0 \\ 0 & \frac{1}{2} \end{bmatrix} x \quad \text{scaled by } \frac{1}{2}$$

$$f_2(x) = \begin{bmatrix} \frac{1}{2} & 0 \\ 0 & \frac{1}{2} \end{bmatrix} x + \begin{bmatrix} \frac{1}{2} \\ 0 \end{bmatrix} \quad \text{scaled by } \frac{1}{2}$$

$$f_3(x) = \begin{bmatrix} \frac{1}{2} & 0 \\ 0 & \frac{1}{2} \end{bmatrix} x + \begin{bmatrix} \frac{1}{4} \\ \frac{\sqrt{3}}{4} \end{bmatrix} \quad \text{scaled by } \frac{1}{2}$$

Applying the iterated function system to $S(1)$ will produce $S(2)$. Applying it to $S(2)$ will give $S(3)$. The Sierpinski triangle is the attractor for this iterated function system. Hence, if we apply the system repeatedly, starting at $S(0)$, the resulting images will converge to create the Sierpinski triangle.

5.6 Iterated function system of the Sierpinski Carpet_[10]

When constructing the Sierpinski carpet, we start with a square $C(0)$ and we divide it into 9 smaller congruent squares. In the same manner as the Sierpinski triangle, we remove the interior of the square in the centre, leaving us with $C(1)$. In the next iteration, we subdivide the remaining 8 squares each into 9 smaller congruent squares without the centre square, forming $C(2)$. After infinite iterations we obtain the Sierpinski carpet. This process is shown below:

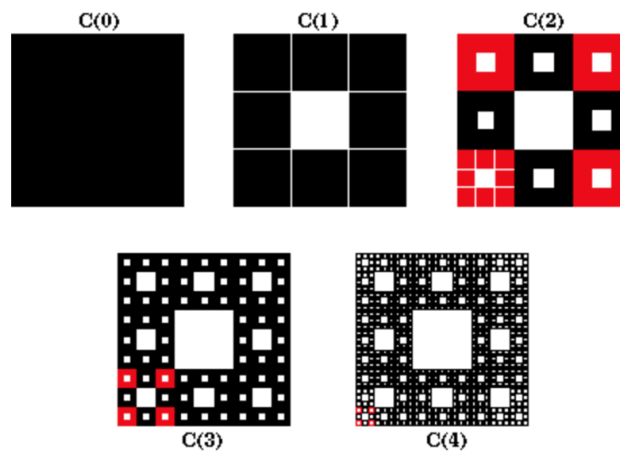


Figure 20: Iterations of the Sierpinski Carpet_[10]

If we take $C(0)$ to be a unit square in which the opposite corners are at $(0,0)$ and $(1,1)$, then the iterated function system would be as follows:

$$f_1(x) = \begin{bmatrix} \frac{1}{3} & 0 \\ 0 & \frac{1}{3} \end{bmatrix} x$$

$$f_2(x) = \begin{bmatrix} \frac{1}{3} & 0 \\ 0 & \frac{1}{3} \end{bmatrix} x + \begin{bmatrix} 0 \\ \frac{1}{3} \end{bmatrix}$$

$$f_3(x) = \begin{bmatrix} \frac{1}{3} & 0 \\ 0 & \frac{1}{3} \end{bmatrix} x + \begin{bmatrix} 0 \\ \frac{2}{3} \end{bmatrix}$$

$$f_4(x) = \begin{bmatrix} \frac{1}{3} & 0 \\ 0 & \frac{1}{3} \end{bmatrix} x + \begin{bmatrix} \frac{1}{3} \\ 0 \end{bmatrix}$$

$$f_5(x) = \begin{bmatrix} \frac{1}{3} & 0 \\ 0 & \frac{1}{3} \end{bmatrix} x + \begin{bmatrix} \frac{1}{3} \\ \frac{2}{3} \end{bmatrix}$$

$$f_6(x) = \begin{bmatrix} \frac{1}{3} & 0 \\ 0 & \frac{1}{3} \end{bmatrix} x + \begin{bmatrix} \frac{2}{3} \\ 0 \end{bmatrix}$$

$$f_7(x) = \begin{bmatrix} \frac{1}{3} & 0 \\ 0 & \frac{1}{3} \end{bmatrix} x + \begin{bmatrix} \frac{2}{3} \\ \frac{1}{3} \end{bmatrix}$$

$$f_8(x) = \begin{bmatrix} \frac{1}{3} & 0 \\ 0 & \frac{1}{3} \end{bmatrix} x + \begin{bmatrix} \frac{2}{3} \\ \frac{2}{3} \end{bmatrix}$$

The Sierpinski carpet is made up of eight exactly self-similar pieces, corresponding to the functions in the iterated function system.

6 Conclusion

We have seen in this thesis how the concept of fractal dimension can be used to describe the appearance of fractals, supported by illustrative examples. For instance, the dimension of the middle third Cantor set is 0.6309, while the dimension of the Sierpinski triangle is 1.58496. This large difference in dimension is expected, considering the great difference in appearance; the Sierpinski triangle is full of holes, whereas the Cantor set is a set of disconnected lines. We also discussed possible limitations of fractal dimension.

Using the same examples, we touched on self-similarity by describing for each of them, how self-similarity works in terms of equations and transformations. The coastline is seen as statistically self-similar and is an application of fractals that exist in the real world. In this thesis, we described the work of Mandelbrot and Richardson. In particular, we focused on the Richardson effect, which showed us that on a logarithmic plot, the relationship between the length of scale and estimated length is linear with a negative slope. We have also seen ideas of how the coastline can be modelled using fractals and fractal concepts, specifically using the Koch curve and fractional Brownian motion, which are both seen as self-similar models.

Lastly, we introduced iterated function systems, and gave illustrated examples of how they can be used to construct fractals. Namely, the Koch curve and Sierpinski triangle, as well as the Koch snowflake and Sierpinski carpet. We can see similarities in the iterated function systems of the Koch curve and Koch snowflake, particularly in the matrix component of their function systems. This is expected, since their structures are very similar; the Koch snowflake is constructed using the development of the Koch curve. On the other hand, the iterated function systems of the Sierpinski triangle and Sierpinski carpet are very different, this is also evident in their differing structures. While the same process is used to create holes in them both, the Sierpinski triangle is made up of triangle holes, whereas the Sierpinski carpet is concerned with square holes.

Bibliography

- [1] Alex Clark. *Chaos and Fractals Lecture Notes, Chapter 6*. Queen Mary, University of London, 2020.
- [2] Kenneth Falconer. *Fractal Geometry: Mathematical Foundations and Applications, Chapter 9*. Third edition.
- [3] Kenneth Falconer. *Fractals: A Very Short Introduction, Chapter 2*. Oxford University Press, 2013.
- [4] Kenneth Falconer. *Fractals: A Very Short Introduction, Chapter 3*. Oxford University Press, 2013.
- [5] Kenneth Falconer. *Fractals: A Very Short Introduction, Chapter 5*. Oxford University Press, 2013.
- [6] Jay Kappraff. The geometry of coastlines: a study in fractals. *Computers Mathematics with Applications*, 312B:655–671, 1986.
- [7] Benoît Mandelbrot. *The Fractal Geometry of Nature, Chapter 5*. W. H. Freeman and Co, 1982.
- [8] Larry Riddle. *Classic Iterated Function Systems, Koch Curve*. Agnes Scott College, 2020.
- [9] Larry Riddle. *Classic Iterated Function Systems, Koch Snowflake*. Agnes Scott College, 2020.
- [10] Larry Riddle. *Classic Iterated Function Systems, Sierpinski Carpet*. Agnes Scott College, 2020.
- [11] Larry Riddle. *Classic Iterated Function Systems, Sierpinski Gasket*. Agnes Scott College, 2020.